frontiers | Frontiers in Earth Science

ORIGINAL RESEARCH
published: 11 April 2022
doi: 10.3389/feart.2022.876401

Experimental Study of Dynamic Characteristics of Tailings With Different Reconsolidation Degrees After Liquefaction

Wensong Wang[1,2], Guansen Cao[2,3], Ye Li[1], Yuxi Zhou[1], Ting Lu[2], Ya Wang[2] and Binbin Zheng[4]*

[1]State Key Laboratory of Geohazard Prevention and Geoenvironment Protection, Chengdu University of Technology, Chengdu, China, [2]State Key Laboratory of Coal Mine Disaster Dynamics and Control, Chongqing University, Chongqing, China, [3]Zijin Mining Company Limited, Shanghang, China, [4]School of Management Science and Engineering, Shandong Technology and Business University, Yantai, China

OPEN ACCESS

Edited by:
Wen Nie,
Jiangxi University of Science and Technology, China

Reviewed by:
Fujiao Tang,
Harbin Institute of Technology, China
Peng Feng,
Chengdu University, China
Changbo Du,
Liaoning Technical University, China

***Correspondence:**
Guansen Cao
caogs_zijin@163.com

Specialty section:
This article was submitted to Geohazards and Georisks, a section of the journal Frontiers in Earth Science

Received: *15 February 2022*
Accepted: *16 March 2022*
Published: *11 April 2022*

Citation:
Wang W, Cao G, Li Y, Zhou Y, Lu T, Wang Y and Zheng B (2022) Experimental Study of Dynamic Characteristics of Tailings With Different Reconsolidation Degrees After Liquefaction. Front. Earth Sci. 10:876401. doi: 10.3389/feart.2022.876401

The construction period of most tailing ponds generally lasts for more than 10 years or even decades. During this period, it may be affected by more than one earthquake and is often subjected to vibrations generated by mining activities. The tailings liquefied by earthquakes or vibrations may experience dynamic loads again. Due to the low permeability of tailings, the reconsolidation process of tailings after liquefaction is prolonged. Therefore, changes in the nature of the tailings caused by previous earthquakes will affect the performance of the tailing dam in the subsequent earthquakes. Dynamic triaxial tests and bending element tests were conducted on two kinds of tailings from a copper mine in Southwest China to study this process. The tailing specimens will undergo two consolidation processes and subsequent cyclic loads during the test. The influence of reconsolidation degree, confining pressure, and particle size on the dynamic characteristics and wave velocity of the tailings after liquefaction under cyclic loading was measured. The results show that the reconsolidation degree significantly affects the trend of the excess pore water pressure ratio changing with the increase in the cycle number of loads. The reconsolidation process after liquefaction of tailings will improve its liquefaction resistance. The relationship between the ratio of the cycle number of liquefaction after reconsolidation to the cycle number of first liquefaction and the reconsolidation degree is proposed. In the entire experimental process, the shear wave velocity of the tailings gradually decreases when applying the cyclic load and gradually increases during the consolidation process, including the first consolidation before cyclic loading and reconsolidation after liquefaction. The research results are of great significance to the safe disposal of tailings, especially those in earthquake-prone areas.

Keywords: tailings, dynamic characteristic, liquefaction, consolidation degree, wave velocity, earthquake

1 INTRODUCTION

A tailing pond is formed by the accumulation of tailings discharged from metal and non-metal mines, which has a high potential risk of debris flow (Vick, 1990; Wei et al., 2013). Once a tailing pond is damaged, it will lead to vast environmental pollution along with casualties and property losses (Villavicencio et al., 2014; Martin-Crespo et al., 2015; Santamarina et al., 2019; Chen et al., 2021). According to relevant statistics, seismic liquefaction is the second significant factor responsible for the failure of a tailing pond (Rico et al., 2008). The laboratory test is a meaningful way to explore the dynamic characteristics of tailings, which can provide a basis for revealing the seismic instability mechanism of tailing dams. Several scholars have studied the dynamic characteristics of tailings such as cyclic shear stress ratio (*CSR*), dynamic shear modulus (G_d), initial shear modulus (G_0), damping ratio (λ_d), shear wave velocity (V_s), and excess pore water pressure (μ_d), etc (Wijewickreme et al., 2005; James et al., 2011; Liu et al., 2012; Cao et al., 2019; Lu et al., 2021).

The collapse of some dams is not due to seismic loading during an earthquake but rather due to reduction in shear strength or liquefaction resistance after an earthquake. The construction period of a tailing pond continues for dozens of years, during which it may have to withstand several accidental earthquakes. The influence of earthquakes on tailing dams is very complicated. The changes in the nature of tailings caused by the previous earthquake will affect the performance of the tailing dam during the subsequent earthquake. The Kayakari tailing reservoir in Japan did not suffer damage in the major earthquake of 2003, while in the minor earthquake of 2011, liquefaction occurred, and the dam broke. Ishihara et al. (2015) have conducted a series of *in situ* experiments and established relevant models for verification. The results show that the overall stability of the tailing dam decreases to some extent even if the earthquake does not directly destroy the dam; however, the strength of the tailings and the stability of the tailings reservoir will increase with the increase of time after the earthquake and reconsolidation of the tailings with the dissipation of excess pore pressure. Therefore, in addition to focusing on whether the dam will be damaged in the earthquake, the research on the dynamic stability of the tailing dam should also pay attention to whether or when the post-earthquake tailing dam can recover to the pre-earthquake stability, that is, the post-earthquake tailing consolidation to what extent can restore the original strength. It is of great significance to study the change in mechanical properties during the reconsolidation process of tailings after an earthquake.

Some researchers have studied the post-liquefaction behavior of sand, silt, and clay with various factors, including densities, fine content, and reconsolidated degrees (U_{re}). Ashour et al. (2009) presented equations to assess the undrained response of liquefied sand based on drained test behavior, indicating that the post-cyclic excess pore pressure and associated residual effective confining pressure govern the post-liquefaction undrained behavior of sand. Wang et al. (2013) studied the effect of limited excess pore pressures on silt, indicating that an excess pore pressure ratio of greater than 0.70 was a prerequisite for significant volume reduction, and thus an increase in undrained shear strength due to reconsolidation after cyclic loading. Soroush and Soltani-Jigheh (2009) measured the behavior of clay under monotonic, cyclic, and post-cyclic loading and found that during post-cyclic monotonic shearing, the clay behaves similarly to over-consolidated soil; the larger the particle size is, the higher the over-consolidation ratio would be. According to previous studies, the dynamic and mechanical properties of post-liquefied soil are affected by factors such as effective confining pressure ($\sigma_c^{'}$), U_{re}, *CSR*, particle size, and other factors. However, most scholars focused more on the residual strength and deformation characteristics of post-liquefied soils with a monotonic shear method and seldom paid attention to the liquefaction resistance with recyclic loading. Tailing dams usually contain a lot of fine grains, resulting in poor permeability, which will make them more prone to liquefaction and collapse (Karim and Alam, 2014). Therefore, it is necessary to study the dynamic response of post-liquefied tailings under cyclic loading during the reconsolidation process under the influence of multifactor coupling.

In this study, a dynamic triaxial test system was adopted to carry out the cyclic loading test again on the tailing specimens with different degrees of reconsolidation after the first liquefaction and the second liquefaction was achieved. Several cyclic loading tests with different U_{re}, $\sigma_c^{'}$, and *CSR* were conducted on two types of tailing specimens. This study aims to obtain the change in excess pore water pressure and shear wave velocity during the cyclic reloading process with variant U_{re}. In particular, the liquefaction resistance of tailings under different U_{re} was compared. The research results can provide a basis for further understanding of the stability change law and failure mechanism of tailing dams in earthquake-prone areas.

2 TEST MATERIALS, METHODS, AND PROCEDURES

2.1 Source of Test Materials

The tailing materials being examined in this study are chosen from the Xiaodae copper tailing pond located 2.8 km in the southwest of Huili County, Liangshan Prefecture, Sichuan Province, China, as shown in **Figure 1**. The Xiaodae tailing pond is surrounded by mountains in three directions, with the bottom of the terrain shaped like a "V." The north side of the terrain is higher than the south, with the slope being 8–10. The total dam height is 187.5 m, and its total final capacity is 953.61 million m^3. It is a typical upstream tailing pond.

The Xiaodae tailing pond is located in the Himalayan earthquake zone. The Himalayan earthquake zone is one of the largest earthquake areas in China and the region where earthquakes occur most intensely and frequently. In the vicinity of the Xiaodae tailing pond, the 7.7 magnitude Tonghai earthquake (5 January 1970), 7.0 magnitude Lijiang earthquake (3 February 1996), 8.0 Wenchuan earthquake (12 May 2008), and 7.0 magnitude Yaan earthquake (20

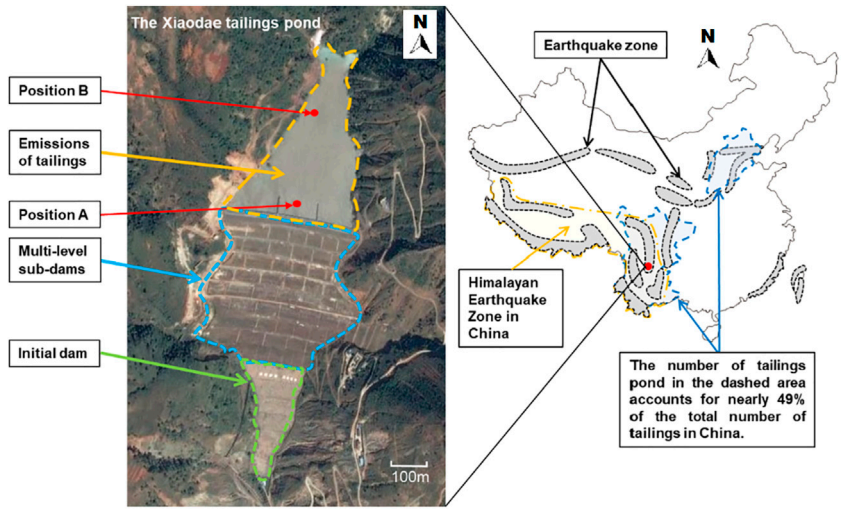

FIGURE 1 | Distribution of the main seismic belt of China and location of the Xiaodae tailing pond.

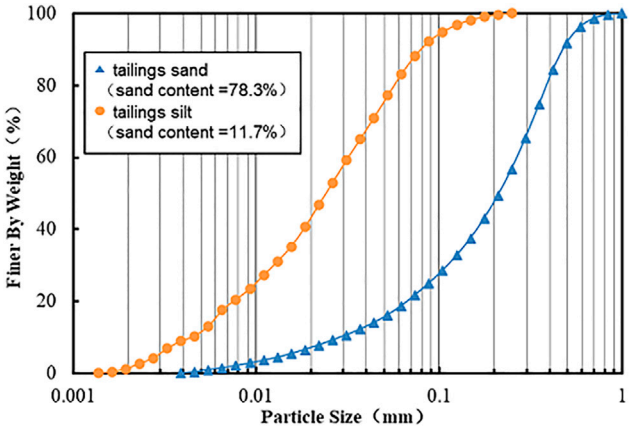

FIGURE 2 | Particle size distribution of the tailings.

April 2013) have occurred. China's seismic belt and mineral resource distribution area have considerably overlapped. There are currently about 8,000 tailing ponds in China, nearly half of which are distributed in the two major earthquake areas (North China and Southwest China) shown in **Figure 1**. Therefore, it is necessary to study the dynamic characteristics of the Xiaodae tailings for variant consolidation degrees after cyclic loading.

2.2 Physical and Mechanical Properties of Test Materials

2.2.1 Particle Size Distribution

The Xiaodae tailing pond is constructed using the upstream method. Therefore, on the top beach surface near the sub-dams, the particle size of the tailings is larger; whereas, at the tail part of the beach, it is finer. Previous studies have shown that particle size has a great effect on the dynamic properties of soils (Gratchev et al., 2006; Yilmaz et al., 2008). Therefore, on the typical top beach surface shown in **Figure 1**, two Xiaodae copper tailings were collected, taken from the front position (position A) and tail position (position B). The particle size distribution curves of tailings were obtained by using an S3500 light-scattering particle size analyzer (manufactured by Microtrac, Inc., Montgomeryville, PA, United States) and shown in **Figure 2** and **Table 1**. The clay content (particle size $\leq$ 0.005 mm), silt content (0.005 mm $<$ particle size $\leq$ 0.074 mm), and sand content (particle size $>$ 0.074 mm) in the coarse tailings in the test are 0.9, 20%, 20.8%, and 78.3%, respectively. The abovementioned particle contents in fine tailings are 13.1%, 75.2%, and 11.7%, respectively. Both tailings have a uniformity coefficient greater than 5 and a curvature coefficient between 1 and 3, so they are both granular materials with good particle gradation. The mineralogy and chemical composition of the tailings have been described in detail in our published article (Cao et al., 2019).

2.2.2 Static Characteristics

According to the National Standard of the People's Republic of China "Standards for Geotechnical Test Methods" (GB/T 50123–2019), the physical properties and static mechanical properties of two tailings were obtained by tests, including density, moisture content, liquid and plastic limit, cohesion, and internal friction angle, as listed in **Table 2**. According to another National Standard of the People's Republic of China "Safety Regulation for Tailings Pond" (GB 39496–2020), the test results show that the two types of tailings can be named tailing sand and tailing silt.

2.2.3 Dynamic Characteristics

The dynamic characteristic parameters of soil usually include liquefaction resistance, shear modulus, and damping ratio. The dynamic characteristics of the test tailings were obtained by dynamic triaxial tests. Generally, liquefaction resistance is

TABLE 1 | Particle size distribution parameters of the tailings.

Category	Clay content (%)	Silt content (%)	Sand content (%)	D_{50} (mm)	C_u	C_c
Tailing sand	0.9	20.8	78.3	0.024	9.66	1.74
Tailing silt	13.1	75.2	11.7	0.211	7.75	1.36

D_{50} refers to the average particle size, C_u refers to the uniform coefficient, and C_c refers to the curvature coefficient.

TABLE 2 | Physical property and static mechanical property parameters of the tailings.

Category	Specific gravity	Dry density (g/cm^3)	Void ratio *e*	Natural moisture content (%)	Effective cohesion *c* (kPa)	Effective internal friction angle φ (°)	Liquid limit (%)	Plastic limit (%)
Tailings sand	2.85	1.51	0.89	12	7	34	22	17
Tailings silt	2.86	1.54	0.86	15	12	29	24	18

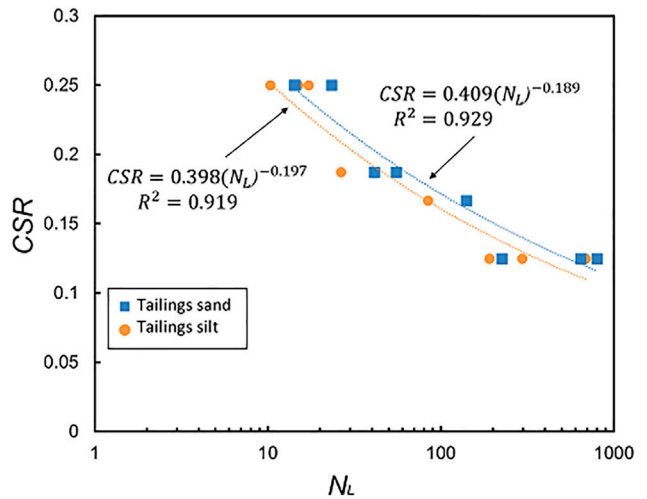

FIGURE 3 | Number of liquefaction failure cycles (N_L) versus the cyclic shear stress ratio (*CSR*) of the tailings.

expressed by the relationship between the *CSR* and number of liquefaction failure cycles N_d, as given in **Eqs 1**, **2** (Lu et al., 2021).

$$CSR = \tau / \sigma_c^{'}, \tag{1}$$

$$CSR = a \cdot N_d^b, \tag{2}$$

where τ and $\sigma_c^{'}$ are shear stress and effective confining pressure, respectively; a and b are the fitting parameters that depend on some common factors of tailings such as density, particle structure and size, stress history, etc. The results of the liquefaction resistance are shown in **Figure 3**. Comparing the experimental results of the liquefaction resistance of the tailing sand and tailing silt, it can be seen that the empirical equation **Eq. 2** can fit well in the relationship between the *CSR* and failure cycle number of tailings.

The dynamic deformation characteristics of soil are usually expressed by the relationship between the dynamic shear modulus ratio (G_d/G_0)/damping ratio (λ_d) and dynamic shear strain (γ_d). G_d, G_0, and λ_d can be obtained by analyzing the hysteresis curve and shear wave velocity (Lu et al., 2021). In **Figure 4**, G_d/G_0~γ_d and λ_d~γ_d of the test tailings were compared to previous relevant findings on natural sands (Seed and Idriss, 1970; Ishihara, 1996; Rollins et al., 1998; Stokoe et al., 2004). It can be seen from **Figure 4** that compared with natural sand, the dynamic shear modulus ratio and damping ratio of tailings are more sensitive to changes in dynamic shear strain. When the dynamic shear strain exceeds 0.001, compared with the natural sand, the attenuation of the dynamic shear modulus ratio and increase of the damping ratio of the tailings are both faster; especially when the dynamic shear strain exceeds 0.01, the damping ratio of the tailings will be significantly larger than that of natural sand. The abovementioned phenomenon reflects the particularity of the dynamic behavior of tailings under cyclic loading.

2.3 Test Methods and Procedures

All tests in the study were performed in stress-controlled loading mode on a DYNTTS-type dynamic triaxial instrument (manufactured by GDS Instruments, Hampshire, United Kingdom). The loading waveform is controlled by a servo system as a sine wave with a vibration frequency of 1 Hz. The tailings specimens were prepared by following the requirements of the Standards for Geotechnical Test Methods (GB/T 50123-2019). The samples collected from the Xiaodae tailing pond were reconstructed into cylindrical specimens with diameter of 50 mm and height of 100 mm using the wet tamping method. The test specimens were prepared according to the dry density and natural moisture content listed in **Table 2**. After the specimen preparation was completed, vacuum saturation was first conducted, and then the multistage back pressure saturation in the pressure chamber was performed until the saturation degree reached 95%. The specimens were subjected to the first consolidation under different confining pressures (100 kPa, 200 kPa, and 400 kPa), and the pore water pressure dissipated to 0 kPa as the consolidation was completed. It should be pointed out that, considering that the liquefaction depth of tailing dam during

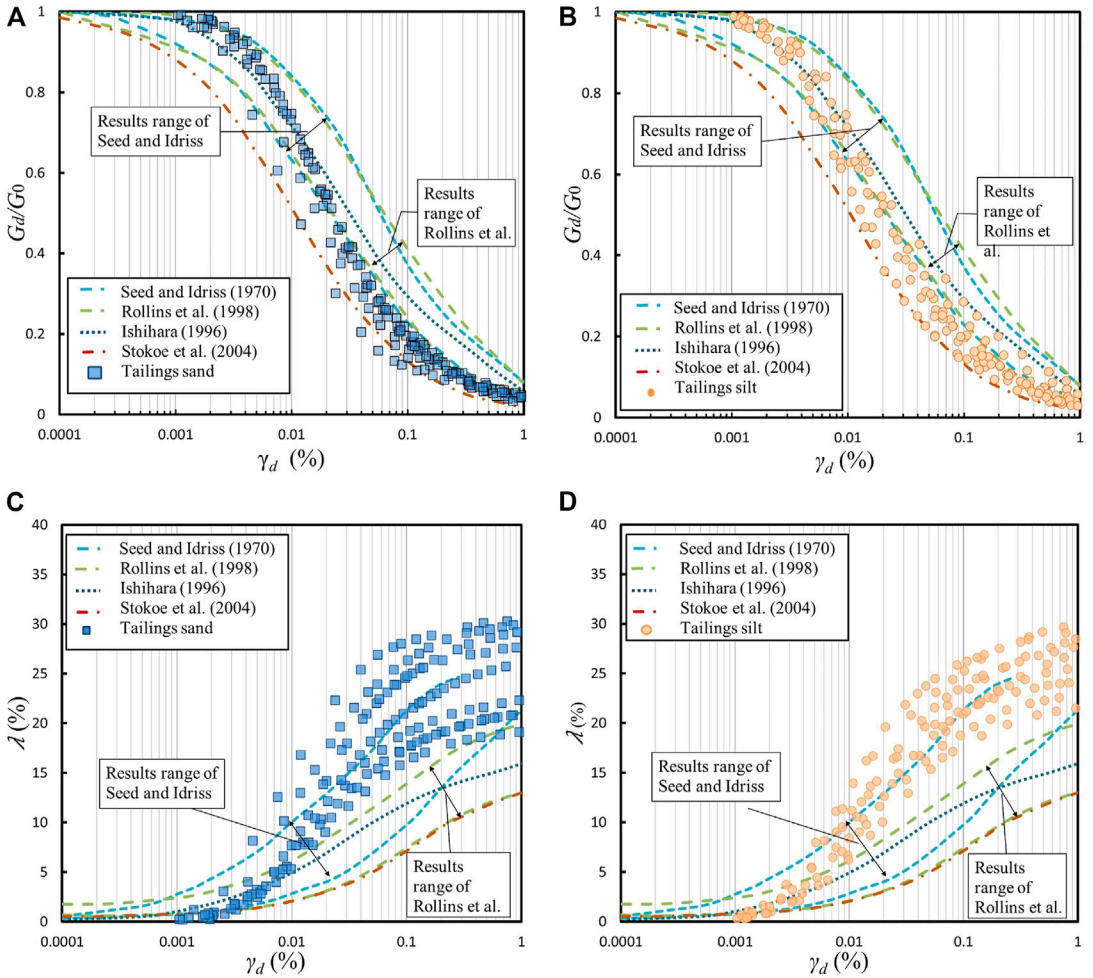

FIGURE 4 | Comparison of the dynamic deformation characteristics of the tailings and natural sands: **(A)** G_d/G_0~γ_d curves of the tailings sand; **(B)** G_d/G_0~γ_d curves of the tailings silt; **(C)** λ_d~γ_d curves of the tailings sand; and **(D)** λ_d~γ_d curves of the tailings silt.

earthquakes generally does not exceed 20 m, the maximum confining pressure in the test was set to 400 kPa, which corresponds to the maximum principal stress at a depth of 20 m.

During the loading stage, cyclic loading of specific *CSR*s was applied to the tailing specimens until the excess pore water pressure was equal to the effective confining pressure, thereby obtaining the liquefied specimens. This process stimulates the liquefaction of tailings caused by earthquakes. Then, the specimens were reconsolidated, that is, being consolidated again. During the reconsolidation process, the excess pore water pressure was controlled to reach a preset U_{re} in order to simulate different stages of the pore water migration and dissipation process at the site after an earthquake. After reconsolidation, the second cyclic loading with the same *CSR*s as the first loading was applied to the specimens. When the excess pore water pressure reached the confining pressure again, the reloading process ended. The shear wave velocity was measured by the bender element test after each consolidation was completed. The data such as the number of loading cycles, axial strain, pore water pressure, and shear wave velocity were collected and recorded in real time during the test process. The detailed

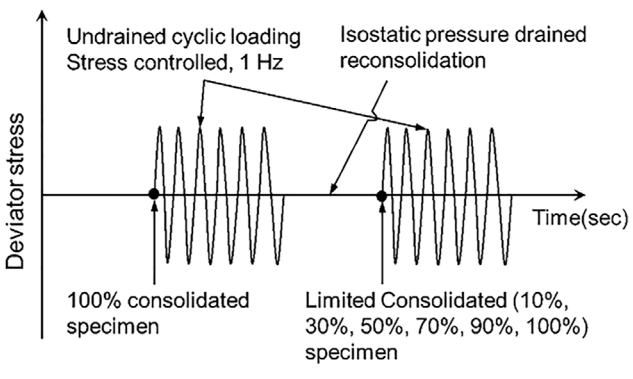

FIGURE 5 | Loading scheme for the dynamic characteristic test of liquefied tailings.

TABLE 3 | Test scheme for dynamic characteristics of liquefied tailings.

Test number	Sample category	Effective confining pressure (kPa)	Cyclic shear stress ratio	Vibration frequency (Hz)	Degree of reconsolidation (%)
M1	Tailings sand	100	0.25	1	20, 40, 60, 80, 100
M2	Tailings sand	200	0.25	1	20, 40, 60, 80, 100
M3	Tailings sand	400	0.25	1	20, 40, 60, 80, 100
M4	Tailings sand	400	0.188	1	10, 30, 50, 70, 90, 100
M5	Tailings silt	100	0.25	1	20, 40, 60, 80, 100
M6	Tailings silt	400	0.188	1	10, 30, 50, 70, 90, 100

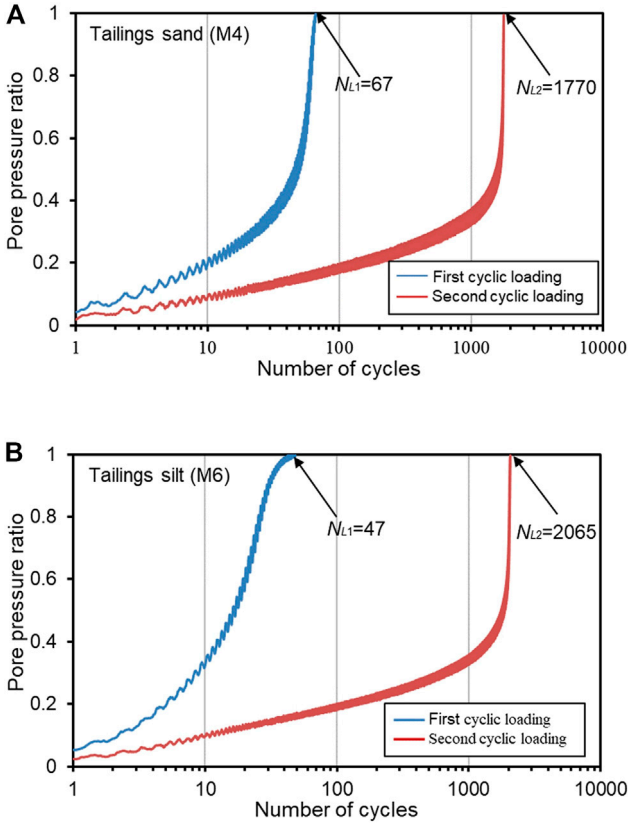

FIGURE 6 | Relationship between the excess pore water pressure ratio and the number of cycles during the two cyclic loading of tailings under full consolidation: **(A)** tailing sand (M4) and **(B)** tailing silt (M6).

experimental scheme and testing process are shown in **Figure 5** and **Table 3**.

3 RESULT ANALYSIS AND DISCUSSION

3.1 Excess Pore Water Pressure

Considering the M4 and M6 test groups as examples, the changes of excess pore water pressure of tailing sand and tailing silt after liquefaction under the cyclic reloading were analyzed. The $\sigma_c^{'}$ and *CSR* in the two groups of tests were both 400 kPa and 0.188, respectively. In this study, the number of liquefaction failure cycles in the two cyclic loading processes was defined as N_{L1} and N_{L2}, respectively.

Figure 6 shows the relationship between the excess pore water pressure ratio ($\mu_d/\sigma_c^{'}$) and number of cycles for the tailing sand and tailing silt during the two cyclic loading processes. After the liquefied tailings are fully consolidated again, the number of liquefaction failure cycles is significantly larger than the original one. This is due to the increased compaction of the tailings due to vibration and subsequent drainage consolidation (Geng et al., 2021). The liquefaction number of tailing silt increased from 67 to 1770 and that of tailing silt increased from 47 to 2065. That is, compared with tailing sand, the effect of the first vibration on the liquefaction resistance of tailing silt was more significant. This phenomenon reflects that after the tailings are subjected to dynamic loads such as earthquakes if they are sufficiently consolidated, their liquefaction resistance will be enhanced. Meanwhile, the effect of the vibro-consolidation method in the process of tailing dam construction is also confirmed.

The relationship between the excess pore water pressure ratio and number of cycles of tailings after liquefaction with different U_{re} is shown in **Figure 7**. **Figure 7** shows that with the increase in the U_{re}, the number of the liquefaction failure cycles increases, indicating an increase in liquefaction resistance. When the U_{re} is low (such as 10%~70% in **Figure 7**), the excess pore water pressure ratio is approximately linear with the logarithm of the number of cycles; when U_{re} is high (such as 90% and 100% in **Figure 7**), the excess pore water pressure ratio is approximately piecewise linear with the logarithm of the number of cycles: with the increase in the cycle numbers, the increase of the excess pore water pressure ratio can be divided into two stages: when the pore pressure ratio is less than 0.5, its increase rate is relatively low; when it exceeds 0.5, the pore pressure ratio increases rapidly. Bi et al. (2016) explained this phenomenon, arguing that the porosity nonuniformity of the particle system affects the occurrence of particle dislocation, and the porosity nonuniformity of the particle system becomes weaker as the pore pressure increases.

The dynamic pore pressure model of soil describes the development law of excess pore water pressure under the action of cyclic loading and is usually expressed by the relationship between the excess pore water pressure ratio and cycle number ratio (the ratio of the number of cycles to the number of liquefaction failures, N/N_L). **Figure 8** shows the dynamic pore pressure models of tailings after liquefaction with different U_{re}. When the U_{re} is low, the dynamic pore

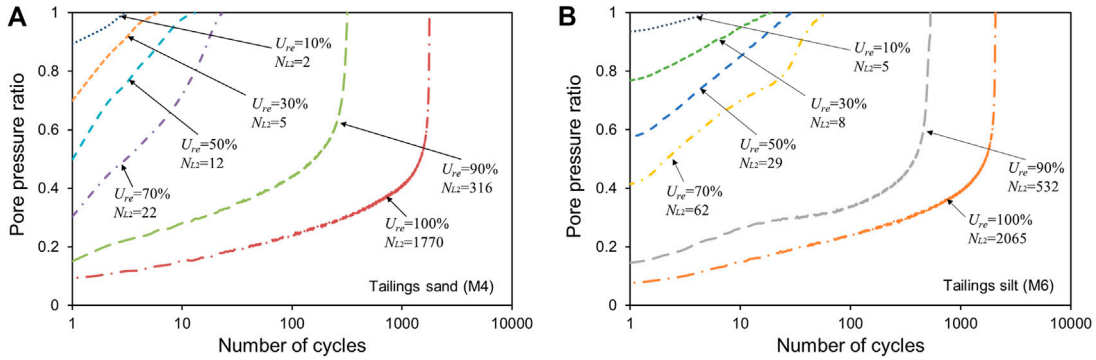

FIGURE 7 | Relationship between the excess pore water pressure ratio and number of cycles of tailings after liquefaction with different reconsolidation degrees (U_{re}): **(A)** tailing sand (M4) and **(B)** tailing silt (M6).

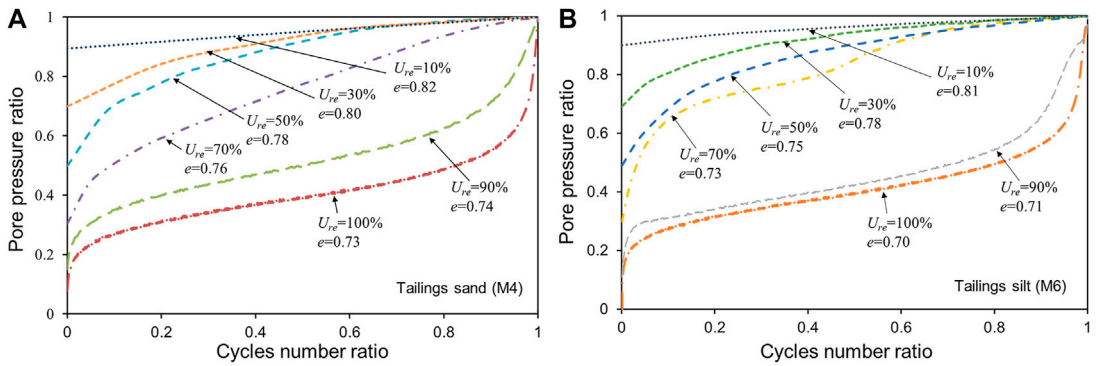

FIGURE 8 | Dynamic pore pressure models of tailings after liquefaction with different reconsolidation degrees (U_{re}): **(A)** tailing sand (M4) and **(B)** tailing silt (M6).

pressure models of the two tailings are both convex type; with the increase of U_{re}, the dynamic pore pressure model gradually evolves into a convex–concave type. **Figure 8** also shows the void ratios corresponding to different U_{re} calculated according to the drainage volume during the reconsolidation drainage process. With the increase of U_{re}, the void ratio gradually decreases, and the particle structure of the tailings changes from a loose state to a dense state, resulting in a change in the shape of the dynamic pore pressure model. The same phenomenon was obtained in the experimental studies of natural sands by Papadopoulou et al. (2010) and Monkul et al. (2015), indicating that tailings have a strong similarity with natural sands in the evolution law of dynamic pore pressure, wherefore it is also prone to liquefaction under vibration.

3.2 Liquefaction Resistance

From the test results of the two cyclic loadings, it can be seen that the reconsolidation effect after the cyclic loading increases the liquefaction resistance of the tailings. The results of a series of experiments conducted by Ishihara et al. (2015) show that while the earthquake reduces the overall stability of the tailing dam in the short term, the strength of the tailings gradually increases over time as reconsolidation effects occur. Similar conclusions are also found in the work of Wang et al. (2013), who studied the undrained shear strength of fully reconsolidated liquefied silt, which was 4.2 times that of the original silt. The ratio of the second liquefaction failure cycle number (N_{L2}) to the first liquefaction failure cycle number (N_{L1}) of the same specimen can quantitatively characterize the influence of the reconsolidation effect on the liquefaction resistance of tailings. In the study, the ratio N_{L2}/N_{L1} is named as the liquefaction cycle number ratio. The liquefaction cycle number ratios of tailings with various U_{re} were calculated, as shown in **Figure 9** and **Eq. 3**.

$$\lg\left(\frac{N_{L2}}{N_{L1}}\right) = A\left(1 - \frac{\mu}{\sigma_c^{'}}\right)^{B} + \lg C, \tag{3}$$

where A, B, and C are the fitting parameters, μ_d is the excess pore water pressure, $\sigma_c^{'}$ is the effective confining pressure, and $1 - \frac{\mu}{\sigma_c^{'}}$ is equal to U_{re}. The results of the fitting parameters are shown in **Table 4**. All the goodness-of-fit of the six groups of test results using **Eq. 3** is close to 1, which confirms the applicability of the formula. When the N_{L2}/N_{L1} is equal to 1, **Eq. 3** implies that the liquefaction resistance of the tailings with this reconsolidation degree returns to that before cyclic loading.

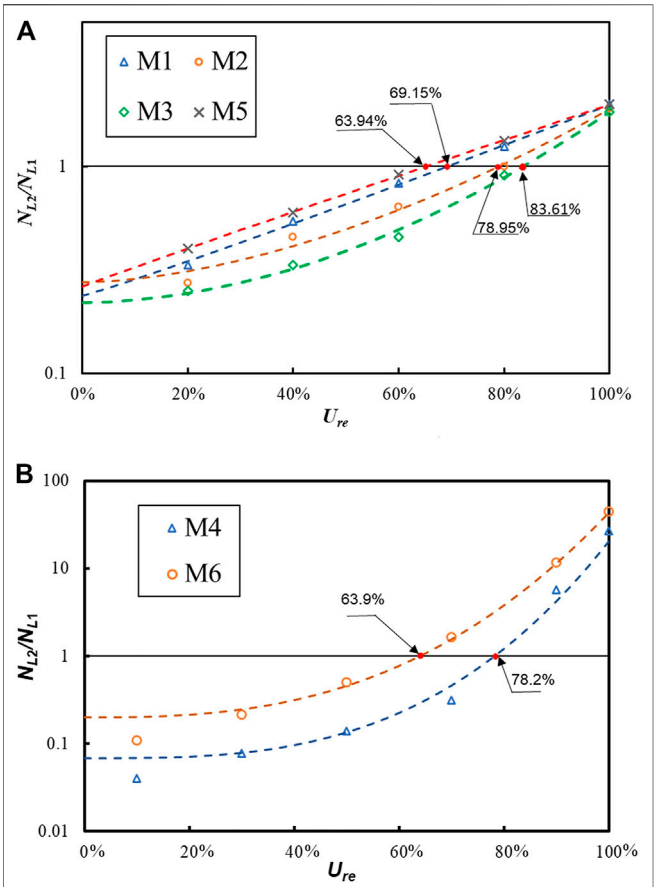

FIGURE 9 | Relationship between the liquefaction cycle number ratio (N_{L2}/N_{L1}) and reconsolidation degrees (U_{re}) of tailings: **(A)** test groups with a *CSR* of 0.25 and **(B)** test groups with a *CSR* of 0.188.

It can be seen from the six sets of experimental results shown in **Figure 9** that all the N_{L2}/N_{L1} increase with the increase of U_{re}. A reasonable explanation for this phenomenon is that the soil skeleton is completely remodeled during the development of liquefaction: although the effective stress is almost zero post liquefaction, the particles are rearranged to form a new skeleton structure with stronger stability potential; during the reconsolidation process, the excess pore water pressure gradually dissipates, the newly formed particle skeleton structure becomes dense and stable, and its liquefaction resistance exceeds that of the original tailings at pre-liquefaction (Wang and Wei, 2016).

The effective confining pressure of the three test groups of M1, M2, and M3 increased gradually, and the other conditions were the same. It can be seen from the data of M1, M2, and M3 in **Figure 9** that with the increase of the effective confining pressure, the N_{L2}/N_{L1} of the liquefied tailings under the same U_{re} gradually decreases. When N_{L2}/N_{L1} is equal to 1, the U_{re} of the three groups of M1, M2, and M3 are 69.15%, 78.95%, and 83.61%, respectively, that is, the U_{re} required to restore the liquefaction resistance before cyclic loading increases with the increase of the effective confining pressure. This may be due to the high confining pressure limiting the extent of particle skeletal structure remodeling during cyclic loading.

TABLE 4 | Fitting results of the relationship between the liquefaction cycle number ratio and reconsolidation degrees of tailings.

Test number	A	B	C	R2
M1	0.926	1.060	0.2365	0.99
M2	0.840	1.709	0.2748	0.97
M3	0.923	1.883	0.2193	0.98
M4	4.176	1.663	0.0018	0.96
M5	0.882	0.971	0.2623	0.99
M6	2.337	2.699	0.2043	0.97

Comparing the results of M1 and M5 in **Figure 9A** and M4 and M6 in **Figure 9B**, we can analyze the difference in the relationship between N_{L2}/N_{L1} and U_{re} of tailing sand and tailing silt. Under the same other conditions, the N_{L2}/N_{L1} of tailing silt is significantly larger than that of tailing sand, indicating that tailing silt has a higher increase in liquefaction resistance than tailing sand after liquefaction and reconsolidation. McDowell and Bolton (1999) proposed that when a granular material has wide disparity in particle size, the small particles are kinematically unstable, and the large particles are stable. Therefore, due to the larger number of fine particles in tailing silt, its particle structure is better optimized after cyclic loading, resulting in its N_{L2}/N_{L1} being higher than that of tailing sand.

Meanwhile, comparing the results of M3 and M4 in **Figure 9** (with different *CSR* and other same conditions), it can be seen that the *CSR* has a significant impact on the shape of the relationship curve between N_{L2}/N_{L1} and U_{re}: the curve with a *CSR* of 0.188 is significantly steeper than that with a *CSR* of 0.25, indicating that a more significant increase in liquefaction resistance can be obtained by applying a cyclic load with a smaller *CSR*.

The N_{L2}/N_{L1} versus U_{re} results of the study provide a new rapid and feasible method for estimating the liquefaction resistances of tailings after an earthquake. By measuring the pore water pressure of the tailings after the earthquake to obtain the U_{re}, combined with the liquefaction resistance of the tailings before the earthquake, the liquefaction resistance of the tailings after the earthquake can be obtained without the need to carry out a large number of dynamic tests again. This has an important guiding significance for the post-earthquake risk assessment and emergency treatment of tailing ponds.

3.3 Shear Wave Velocity

Shear wave velocity is an important index to reflect the dynamic strength and dynamic deformation characteristics of soil (Kayabali, 1996; Rahman and Siddiqua, 2017). Taking the test results of M4 and M6 as examples, the shear wave velocity changes in tailing sand and tailing silt during cyclic loading and drainage consolidation were analyzed, as shown in **Figure 10A**. The shear wave velocities of the two tailings decreased significantly under cyclic loading and gradually recovered during the subsequent reconsolidation process. Many previous studies have shown that there is a strong correlation between the shear wave velocity of soil and its compactness, which can be expressed by void ratio due to the

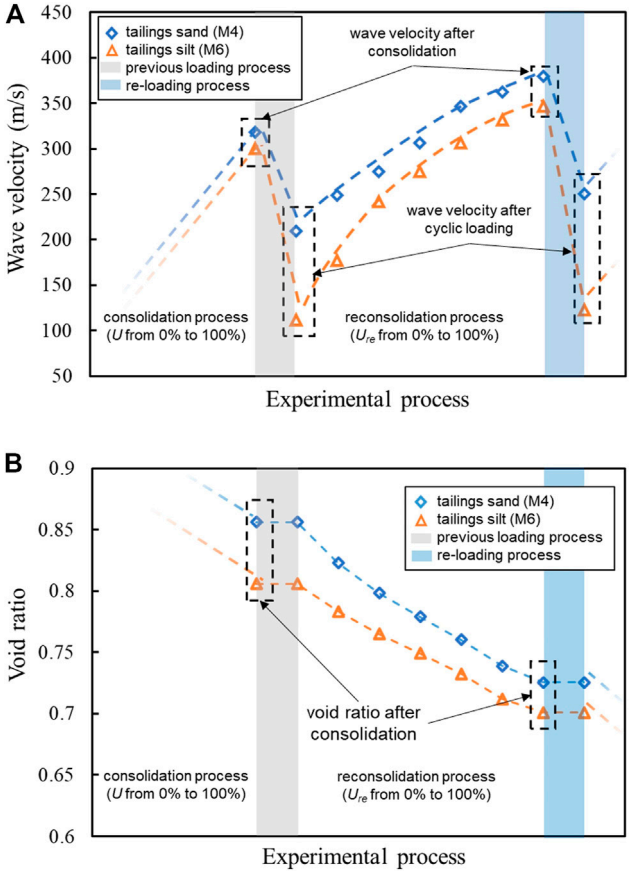

FIGURE 10 | Changes of shear wave velocity and void ratio of tailing sand (M4) and tailing silt (M6) during the test: **(A)** wave velocity and **(B)** void ratio.

different propagation velocities of waves in solids and liquids (Cao et al., 2019; Li et al., 2022). The change in the void ratio of the tailing specimens during the whole test process is shown in **Figure 10B**. During the consolidation process, the particle structure of tailings becomes tighter under confining pressure, the void ratio decreases, and the water in the pores is gradually discharged, resulting in a gradual increase in the shear wave velocity. Since the compactness of the tailings after reconsolidation exceeds that after the first consolidation, the wave velocity of the tailings after reconsolidation is also significantly higher than that after the first consolidation. It is worth noting that the void ratio of the specimen did not change during the two undrained cyclic loadings, but the shear wave velocity still decreased significantly. Whalley et al. (2012) pointed out that the wave velocity of soil is directly related to the effective stress in addition to the compactness: the generation of excess pore water pressure microscopically hinders the direct contact of adjacent particles, thereby increasing the proportion of the liquid medium in the propagation path of the wave. Therefore, under the action of cyclic loading, the increase of excess pore water pressure in the tailings (the decrease of effective stress) leads to the decrease of wave velocity.

Figure 10A also shows that the shear wave velocity of tailing sand is higher than that of tailing silt, and compared with the tailing sand, cyclic loading has a greater effect on the wave velocity of tailing silt. Akbari Paydar and Ahmadi (2016) also found in similar experiments on natural sands of different particle sizes that the higher the content of coarse particles, the higher the wave velocity, although the porosity ratio of sand with larger particle size is relatively lower. This may be because the larger the content of fine particles, the more complex the interlaced structure of particles and pore water, resulting in increased wave propagation time; the contact strength between fine particles is weak, and the contact between fine particles is easily destroyed during cyclic loading so that the proportion of the solid medium in the propagation path of the wave is reduced (Zhang et al., 2015).

4 CONCLUSION

In this study, a variety of dynamic triaxial tests and bending element tests were performed to analyze the dynamic characteristics and wave velocity characteristics of tailing sand and tailing silt with multiple reconsolidation degrees after liquefaction, from which the following conclusions are drawn:

During the process of cyclic reloading of the liquefied tailings, the development law of excess pore water pressure is related to the reconsolidation degree: when the reconsolidation degree is low, the excess pore water pressure ratio and the logarithm of the cycles number are approximately linear, and the dynamic pore pressure model is of convex type; when the reconsolidation degree is high, the excess pore water pressure ratio and the logarithm of the cycles number is approximately piecewise linear (when the excess pore water pressure ratio exceeds 0.5, its growth rate increases significantly), and the dynamic pore pressure model is convex–concave type.

The liquefaction resistance of the tailings increases with the reconsolidation degree and eventually exceeds that of the original tailings. A fitting formula is proposed to characterize the relationship between the reconsolidation degree and liquefaction resistance of reconsolidation tailings. The liquefaction resistance of reconsolidated tailings decreases with the increase of effective confining pressure and particle size, and the decrease of the cyclic shear stress ratio can make the relationship curve between the two liquefaction cycle ratio and reconsolidation degree steeper.

The shear wave velocity of tailings is affected by compaction, effective stress, and particle size. During the drainage consolidation process, the wave velocity increases gradually due to the increase in the compactness of the tailings; in the undrained cyclic loading process, although the compaction of the tailings does not change, the reduction of effective stress will also lead to the reduction of wave velocity. In addition, the effect of cyclic loading on wave velocity is more pronounced with decreasing particle size.

The research results can provide a basis for further understanding of the stability change law and failure mechanism of tailing dams and are of great significance to the safe disposal of tailings in earthquake-prone areas.

DATA AVAILABILITY STATEMENT

The raw data supporting the conclusion of this article will be made available by the authors, without undue reservation.

AUTHOR CONTRIBUTIONS

Conceptualization: WW and GC; data curation: GC and YL; formal analysis: WW, GC and TL; funding acquisition: WW and BZ; investigation: YZ, TL and YW; methodology: GC; project administration: WW; supervision: BZ; validation: YL and YZ; visualization: GC and YZ; writing—original draft: WW and GC; writing—review and editing: WW.

FUNDING

This study was financially supported by the National Natural Science Foundation of China (51804051 and 51804178) and the Natural Science Foundation of Chongqing, China (cstc2019jcyj-bshX0022).

REFERENCES

Akbari Paydar, N., and Ahmadi, M. M. (2016). Effect of Fines Type and Content of Sand on Correlation between Shear Wave Velocity and Liquefaction Resistance. *Geotech Geol. Eng.* 34 (6), 1857–1876. doi:10.1007/s10706-016-9995-8

Ashour, M., Norris, G., and Nguyen, T. (2009). Assessment of the Undrained Response of Sands under Limited and Complete Liquefaction. *J. Geotech. Geoenviron. Eng.* 135 (11), 1772–1776. doi:10.1061/(ASCE)GT.1943-5606.0000114

Bi, Z., Huang, W., Sun, Q., and Sun, S. (2016). Experimental Analysis of Cyclic Loading on a Cohesionless Granular System. *Granular Matter* 18 (1), 10. doi:10.1007/s10035-016-0611-7

Cao, G., Wang, W., Yin, G., and Wei, Z. (2019). Experimental Study of Shear Wave Velocity in Unsaturated Tailings Soil with Variant Grain Size Distribution. *Constr. Build. Mater.* 228, 116744. doi:10.1016/j.conbuildmat.2019.116744

Chen, X., Jing, X., Chen, Y., Pan, C., and Wang, W. (2021). Tailings Dam Break: The Influence of Slurry with Different Concentrations Downstream. *Front. Earth Sci.* 9, 726336. doi:10.3389/feart.2021.726336

Geng, W., Wang, W., Wei, Z., Huang, G., Jing, X., Jiang, C., et al. (2021). Experimental Study of Mesostructure Deformation Characteristics of Unsaturated Tailings with Different Moisture Content. *Water* 13 (1), 15. doi:10.3390/w13010015

Gratchev, I. B., Sassa, K., Osipov, V. I., and Sokolov, V. N. (2006). The Liquefaction of Clayey Soils under Cyclic Loading. *Eng. Geol.* 86 (1), 70–84. doi:10.1016/j.enggeo.2006.04.006

Ishihara, K., Ueno, K., Yamada, S., Yasuda, S., and Yoneoka, T. (2015). Breach of a Tailings Dam in the 2011 Earthquake in Japan. *Soil Dyn. Earthquake Eng.* 68, 3–22. doi:10.1016/j.soildyn.2014.10.010

Ishihara, K. (1996). *Soil Behavior in Earthquake Geotechnics*. Oxford, UK: Clarendon Press.

James, M., Aubertin, M., Wijewickreme, D., and Wilson, G. W. (2011). A Laboratory Investigation of the Dynamic Properties of Tailings. *Can. Geotech. J.* 48 (11), 1587–1600. doi:10.1139/T11-060

Karim, M. E., and Alam, M. J. (2014). Effect of Non-plastic silt Content on the Liquefaction Behavior of Sand-silt Mixture. *Soil Dyn. Earthquake Eng.* 65, 142–150. doi:10.1016/j.soildyn.2014.06.010

Kayabali, K. (1996). Soil Liquefaction Evaluation Using Shear Wave Velocity. *Eng. Geol.* 44 (1-4), 121–127. doi:10.1016/S0013-7952(96)00063-4

Li, J., Kong, L., and Jin, L. (2022). Stress History and Time Effect on Shear Modulus of Expansive Soils. *Arab J. Geosci.* 15 (1), 35. doi:10.1007/s12517-021-09342-y

Liu, H.-m., Yang, C.-h., Zhang, C., and Mao, H.-j. (2012). Study on Static and Dynamic Strength Characteristics of Tailings Silty Sand and its Engineering Application. *Saf. Sci.* 50 (4), 828–834. doi:10.1016/j.ssci.2011.08.025

Lu, T., Wang, W., Wei, Z., Yang, Y., and Cao, G. (2021). Experimental Study on Static and Dynamic Mechanical Properties of Phosphogypsum. *Environ. Sci. Pollut. Res.* 28 (14), 17468–17481. doi:10.1007/s11356-020-12148-2

Martín-Crespo, T., Gómez-Ortiz, D., Martín-Velázquez, S., Esbrí, J. M., de Ignacio-San José, C., Sánchez-García, M. J., et al. (2015). Abandoned Mine Tailings in Cultural Itineraries: Don Quixote Route (Spain). *Eng. Geol.* 197, 82–93. doi:10.1016/j.enggeo.2015.08.008

McDowell, G. R., and Bolton, M. D. (1999). A Micro Mechanical Model for Isotropic Cyclic Loading of Isotropically Clastically Compressed Soil. *Gm* 1 (4), 183–193. doi:10.1007/s100350050024

Monkul, M. M., Gültekin, C., Gülver, M., Akın, Ö., and Eseller-Bayat, E. (2015). Estimation of Liquefaction Potential from Dry and Saturated sandy Soils under Drained Constant Volume Cyclic Simple Shear Loading. *Soil Dyn. Earthquake Eng.* 75, 27–36. doi:10.1016/j.soildyn.2015.03.019

Papadopoulou, A., Kallioglou, P., Tika, T., Papadopoulos, S., and Batum, E. (2010). Liquefaction Resistance of Silty Sands and Dynamic Properties of Cohesive Soils from Düzce, Turkey. *J. Earthquake Eng.* 14 (3), 351–362. doi:10.1080/13632460903387095

Rahman, M. Z., and Siddiqua, S. (2017). Evaluation of Liquefaction-Resistance of Soils Using Standard Penetration Test, Cone Penetration Test, and Shear-Wave Velocity Data for Dhaka, Chittagong, and Sylhet Cities in Bangladesh. *Environ. Earth Sci.* 76 (5), 207. doi:10.1007/s12665-017-6533-9

Rico, M., Benito, G., Salgueiro, A. R., Díez-Herrero, A., and Pereira, H. G. (2008). Reported Tailings Dam Failures. *J. Hazard. Mater.* 152 (2), 846–852. doi:10.1016/j.jhazmat.2007.07.050

Rollins, K. M., Evans, M. D., Diehl, N. B., and Iii, W. D. D. (1998). Shear Modulus and Damping Relationships for Gravels. *J. Geotech. Geoenviron. Eng.* 124 (5), 396–405. doi:10.1061/(asce)1090-0241(1998)124:5(396)

Santamarina, J. C., Torres-Cruz, L. A., and Bachus, R. C. (2019). Why Coal Ash and Tailings Dam Disasters Occur. *Science* 364 (6440), 526–528. doi:10.1126/science.aax1927

Seed, H. B., and Idriss, I. M. (1970). *Soil Moduli and Damping Factors for Dynamic Response Analyses*. Report EERC 70/10. Berkeley, California: University of California. Earthquake Engineering Research Center.

Soroush, A., and Soltani-Jigheh, H. (2009). Pre- and post-cyclic Behavior of Mixed Clayey Soils. *Can. Geotech. J.* 46 (2), 115–128. doi:10.1139/T08-109

Stokoe, K. H., Darendeli, M. B., Menq, F., and Choi, W. K. (2004). "Comparison of the Linear and Nonlinear Dynamic Properties of Gravels , Sands , Silts and Clays," in Proceedings of the 11th International Conference on Soil Dynamics and Earthquake Engineering.

Vick, S. G. (1990). *Planning, Design, and Analysis of Tailings Dams*. Vancouver, BC, Cananda: BiTech Publishers.

Villavicencio, G., Espinace, R., Palma, J., Fourie, A., and Valenzuela, P. (2014). Failures of Sand Tailings Dams in a Highly Seismic Country. *Can. Geotech. J.* 51 (4), 449–464. doi:10.1139/cgj-2013-0142

Wang, G., and Wei, J. (2016). Microstructure Evolution of Granular Soils in Cyclic Mobility and post-liquefaction Process. *Granular Matter* 18 (3), 51. doi:10.1007/s10035-016-0621-5

Wang, S., Luna, R., and Yang, J. (2013). Postcyclic Behavior of Low-Plasticity silt with Limited Excess Pore Pressures. *Soil Dyn. Earthquake Eng.* 54, 39–46. doi:10.1016/j.soildyn.2013.07.016

Wei, Z., Yin, G., Wang, J. G., Wan, L., and Li, G. (2013). Design, Construction and Management of Tailings Storage Facilities for Surface Disposal in China: Case Studies of Failures. *Waste Manag. Res.* 31 (1), 106–112. doi:10.1177/0734242x12462281

Whalley, W. R., Jenkins, M., and Attenborough, K. (2012). The Velocity of Shear Waves in Unsaturated Soil. *Soil Tillage Res.* 125, 30–37. doi:10.1016/j.still.2012.05.013

Wijewickreme, D., Sanin, M. V., and Greenaway, G. R. (2005). Cyclic Shear Response of fine-grained Mine Tailings. *Can. Geotech. J.* 42 (5), 1408–1421. doi:10.1139/T05-058

Yilmaz, Y., Mollamahmutoglu, M., Ozaydin, V., and Kayabali, K. (2008). Experimental Investigation of the Effect of Grading Characteristics on the

Liquefaction Resistance of Various Graded Sands. *Eng. Geol.* 100 (3-4), 91–100. doi:10.1016/j.enggeo.2007.12.002

Zhang, Q., Yin, G., Wei, Z., Fan, X., Wang, W., and Nie, W. (2015). An Experimental Study of the Mechanical Features of Layered Structures in Dam Tailings from Macroscopic and Microscopic Points of View. *Eng. Geol.* 195, 142–154. doi:10.1016/j.enggeo.2015.05.031

Conflict of Interest: Author GC is employed by Zijin Mining Company Limited.

The remaining authors declare that the research was conducted in the absence of any commercial or financial relationships that could be construed as a potential conflict of interest.

Publisher's Note: All claims expressed in this article are solely those of the authors and do not necessarily represent those of their affiliated organizations, or those of the publisher, the editors, and the reviewers. Any product that may be evaluated in this article, or claim that may be made by its manufacturer, is not guaranteed or endorsed by the publisher.